Matlab-Simulink Modelling of 6/4 SRM with Static Data Produced Using Finite Element Method

Fevzi Kentli, Hüseyin Çalik

Department of Electrical Education, Faculty of Technical Education, University of Marmara, 34722-Göztepe, Istanbul, Turkey (e-mail: fkentli@marmara.edu.tr)

Electrical Department of Technical Sciences Vocational College, Istanbul University, 34850-Avcılar, Istanbul, Turkey (e-mail: hcalik@istanbul.edu.tr)

Abstract: The static performance of a switched reluctance motor (SRM) is investigated especially by using the finite element method (FEM) in the design and prototype development steps of the SRM in recent years. In order to determine the real working conditions of the motor, the dynamic behaviour of the SRM should be researched. For this purpose, this study has formed a dynamic model of a 6/4 SRM by using the motor's characteristics, such as inductance, flux and torque obtained by FEM, in Matlab-SIMULINK software. In addition, all the characteristics of the motor are obtained and discussed by using this dynamic model.

Keywords: Switched Reluctance Motor (SRM); Torque; Current Controller; Linear Model

1 Introduction

The switched reluctance motor (SRM) has the advantages of a simple and robust structure, high thermal capability and high speed potential [1, 2]. Commercial products based on SRMs are making their way into the market place. The operational principles of the SRM are quite simple and straightforward, but the proper control of the SRM is not sufficiently completed.

The inherent nonlinearity of a SRM makes torque production highly dependent upon the geometry of the poles, which is characterized by the dependence on both stator current and rotor position. In the past, either a linear or nonlinear model [3-5] with predefined parameters of SRM was used for close-loop control. In spite of the nonlinear nature of the SRM, its linear model represents the dynamic behaviour of SRM with very good approximation. Therefore, for the sake of simplicity, this study represents a linear model of SRM.

In order to produce the maximum torque from a motor at a given speed, the combination of motor – converter should be determined. In general, Computer Aided Design (CAD) tools are employed for this purpose. Some researchers have previously studied in various subjects such as different motor shapes, control strategies and converter types [6, 7], but the studies are not completed and they continue to be discussed in the literature [1-3]. On the other hand, very few simulation studies of the SRM have been achieved with circuit-based languages such as Spice, Simulink, Matrix, Tutsim, Vissim and Mathcad [8, 9].

In this study, a linear dynamic model of 6/4 SRM is generated and the following are examined.

- The dynamic torque ripple of the motor; whether it is in accordance with its static torque ripple or not,
- The amplitude of phase currents to be able to design the driver circuit,
- Dynamic torque, current and flux variations are investigated by applying current control to minimize the torque ripple generated by the motor.

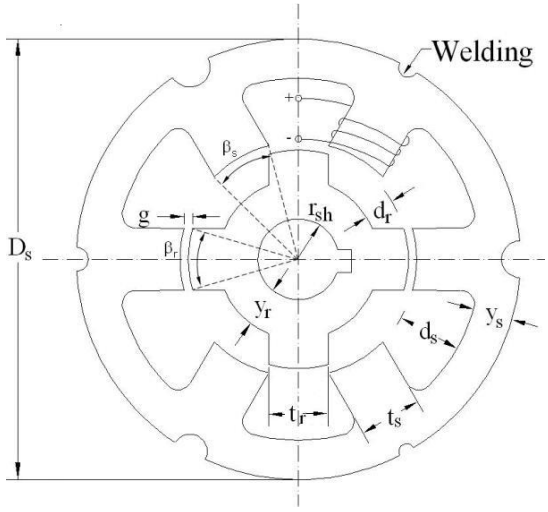

Figure 1
SRM's geometric structure

The geometric structure of the examined motor is given in Fig. 1 and its parameter values are shown in Table I [1]. In dynamic modelling of the 6/4 SRM based on the given specifications, static inductance and torque profiles obtained by the Finite Element Method (FEM) for various current values and 5° rotor angle steps are used [10]. The electrical and mechanical circuit equations are realized by using the Matlab-Simulink program. Mostly, working on a simulink model instead of an actual machine is cheaper, easier and more practical. Also, in some cases, working on a simulink model is a requirement. For example, throughout the manufacturing

of the prototype machine, the machine, just before manufacturing, can be made in the most economic, effective way and with the highest performance by means of changing each parameter on the simulink model in cognizance of machine characteristics such as machine dimensions and the forms of machine parts.

Table I
Motor Parameters [1]

Phase numbers (m) = 3	Shaft radius(r_{sh}) = 0.0087m
Stator pole numbers (N_s) = 6	Rotor pole numbers (N_r) = 4
Stator pole arc (β_s) = 30°	Rotor pole arc (β_r) = 32°
Stator diameter(D_s) = 0.0938 m	Airgap (g) = 0.0002286 m.
Stator pole width(t_s)= 0.0123 m	Rotor pole width(t_r)= 0.0129 m
Stack length (L_{stk}) = 0.047 m	Motor length (L_e) = 0.0762 m
Slot fill factor (k_{sf}) = 33 %	Slot area (A_{slot}) = 0.000309 m^2
Stator slot depth(d_s) = 0.0151m	Rotor slot depth (d_r)= 0.0061m
Stator yoke thickness (y_s) = 0.008178 m.	Rotor yoke thickness (y_r) = 0.008636 m.
J = 0.000189 kgm^2	k_l = 0.005 Nms/rad.
k_f = 0.0001 Nms/rad.	R = 1.11 Ω
P = 450 W	V_s = 24 V

In this study, simulink models of a 6/4 SRM, the parameters and geometrical structure of which are given respectively in Table I and Fig. 1, are obtained as shown in the following figures, and the magnitudes such as the current, flux, torque, and speed of motor are provided by making required data input on these obtained models. As is known, these simulink models can be formed simply by means of a computer.

In this context, a PC-based model in electrical machine design is developed.

1.1 SRM's Linear Models

For various rotor angles, the magnetic flux versus current obtained by FEM is given in Fig. 2. In Fig. 2, the slope of the curve in the linear region without saturation represents the value of the related inductance. The value of inductance varies not only with θ rotating angle, but also with the current through winding due to the saturation feature of magnetic material.

Therefore, the inductance equation in general form can be given as $L = L(\theta,i)$ where θ is the rotor position angle and i is the phase current. Thus, the general expression of total linkage fluxes in the motor becomes as follows.

$$\lambda(\theta,i) = L(\theta,i)\cdot i \tag{1}$$

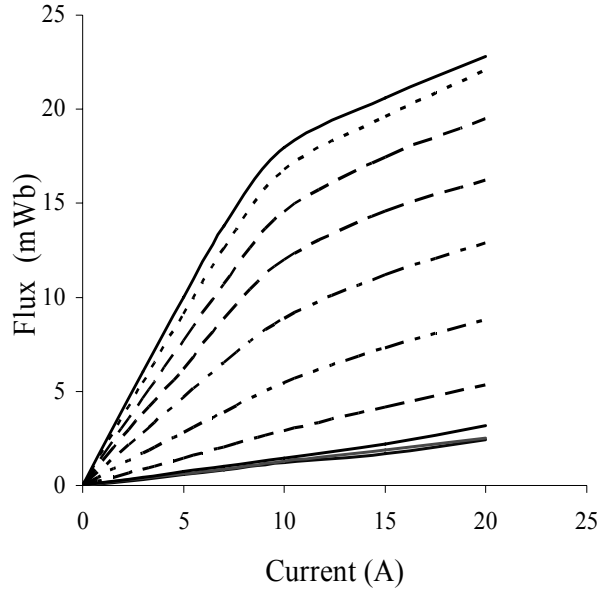

Figure 2
SRM's static flux-current characteristics obtained by using FEM

In this case, if the mutual inductance with short time between the phases is neglected, the winding voltage equation for one phase of SRM can be written as follows.

$$\begin{aligned} V_s &= R\cdot i_s + \frac{d\lambda(\theta,i)}{dt} = R\cdot i_s + \frac{dL(\theta,i)}{dt}\cdot i_s + L(\theta,i)\frac{di_s}{dt} \\ &= R\cdot i_s + \left[L(\theta,i) + \frac{\partial L(\theta,i)}{\partial i}\cdot i_s \right]\frac{di_s}{dt} + \frac{\partial L(\theta,i)}{\partial \theta}\cdot\frac{\partial \theta}{dt}\cdot i_s \end{aligned} \tag{2}$$

where V_s is the winding voltage (V), R is the winding resistance (Ω), i is the winding current (A), $\lambda(\theta,i)$ is the total linkage flux (W_b), $L(\theta,i)$ is the winding inductance (H), θ is the rotor position angle, $(\partial L(\theta,i)/\partial\theta)(\partial\theta/\partial t)\cdot i_s = E$ is the counter (reverse) e.m.f.(V), $\left[L(\theta,i) + \partial L(\theta,i)\cdot i_s / \partial i\right] = L'(\theta,i)$ and the subscribe s is the phase number (like 1,2,3), respectively. Moreover, R and $L(\theta,i)$ values of each phase winding are equal to each other.

Thus, the equivalent circuit for one phase of the SRM is given in Fig. 3. However, in the case of a constant current in the linear model, the total flux expression is given as follows.

$$\lambda(\theta) = L(\theta)\cdot I \tag{3}$$

So, when the rotor with salient-pole aligns with the stator winding, the related winding inductance reaches its maximum value in accordance with the equation of $L = N^2 \cdot \mu \cdot A/l$, where N is the number of turns on the stator winding, μ is the permeability of the magnetic circuit material (H/m), A is the cross-sectional area of the magnetic path (m^2), and l is the average length of the magnetic path (m). L value of the stator winding is only dependent on the rotor angle when the phase current is constant. As seen in Fig. 4, the inductance values are almost constant till 8 A phase current for linear operation in SRM. Thus, it is considered that the winding inductance is only the function of the rotating angle. That is, $L = L(\theta)$. In Fig. 2, the stored energy (W_m) in the magnetic field is represented by the area above the related flux curve and the co-energy (W_m') is represented by the area below the same magnetization curve. As is known, this co-energy is assumed to be the energy that is converted to mechanical energy. The flux-current characteristics in Fig. 2 show that the motor rotates in the linear region till 8 A. In this case, the co-energy equals to the energy stored in the magnetic field in the linear region.

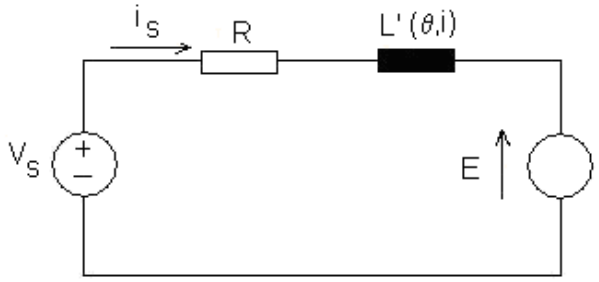

Figure 3
SRM's one phase equivalent circuit

$$W_m = W_m' = \int_0^i \lambda(i,\theta) \cdot di = L(\theta) \cdot i^2 / 2 \tag{4}$$

If the Eq. (4) is rearranged in terms of H and B, Eq. (5) is obtained.

$$W_m = \frac{1}{2} \int H \cdot B \cdot dv \tag{5}$$

where H is the magnetic field intensity (A/m), B is the magnetic flux density (T or Wb/m^2).

The torque equation of the motor can be written by using the co-energy equation because of the relationship between energies as follows.

$$T_e = \partial W_m' / \partial \theta = dL(\theta) \cdot i^2 / (2 \cdot d\theta) \tag{6}$$

where T_e is the motor torque (Nm), i is the winding current (A), and $L(\theta)$ is the winding inductance (H), respectively. The torque is obviously a function of the θ

rotor position angle. As seen in (6), the torque equation is proportional to the square of winding current and independent of the phase current direction. In linear operation, the characteristic of the winding inductance and static torque of motor with respect to the rotor position for one phase are given in Figs. 4 and 5, respectively.

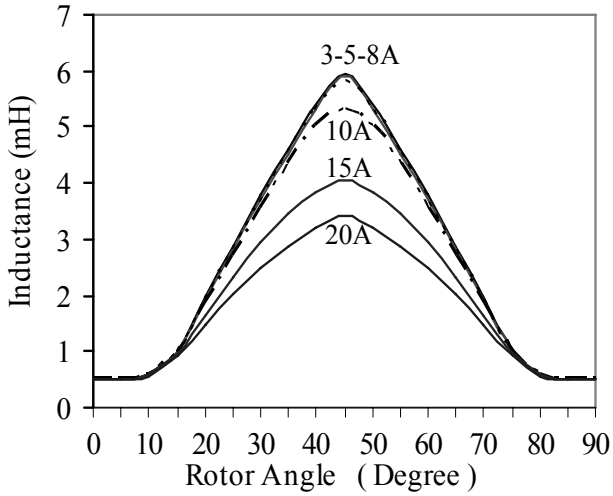

Figure 4
Variation of phase inductance with rotor angle for various phase currents

As shown in Fig. 4, when the angle between the stator pole and rotor pole is at 0° and 90° (unaligned position), the inductance value is at its minimum. In aligned position (at 45°), it has the greatest value. When the rotor pole gets closer to the stator pole, inductance value starts to increase from the minimum value to the maximum, and vice versa.

When in the linear operation, as seen in (6), the produced torque will be constant for the constant current, because the $dL(\theta)/d(\theta)$ ratio is constant. In Fig. 4, the SRM works as a motor by providing positive torque in region (I), and as a generator in region (II) by providing negative torque. In the linear region, however, the inductance slope values remain constant until about 8 A and it decreases for higher current values. Therefore, the motor was assumed to be running within the linear region and the characteristic curve for 8 A was used in obtaining the dynamic model of the SRM.

One of the main purposes of this study is to see the extent to which the static and dynamic characteristic values, such as torques and torque ripples, are in accordance with each other. The static torque characteristic of SRM obtained by using FEM for one phase is presented in Fig. 5. Here, Eqs. (4)-(7) are used to evaluate the values of L and T_e in FEM. The details are given the in appendix.

$$\frac{\partial^2 A}{\partial x^2} + \frac{\partial^2 A}{\partial y^2} = \frac{J_i}{\gamma} = \Re \cdot J_i \tag{7}$$

where $\Re$ is the magnetic resistance (reluctance) ($1/\gamma = \Re$) (1/H or A/Wb), γ is the magnetic conductivity (inverse of $\Re$), A is the vector magnetic potential (Wb/m) and J_i is the current density (A/m^2).

The static torques versus rotor position angle of SRM for the 10 A phase current and three phases are given in Fig. 6.

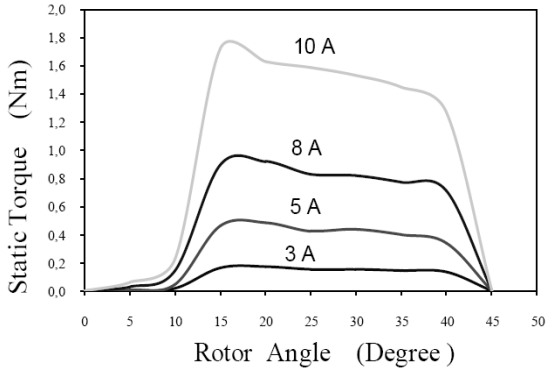

Figure 5

SRM's static torque characteristics obtained by using FEM for one phase and various phase currents

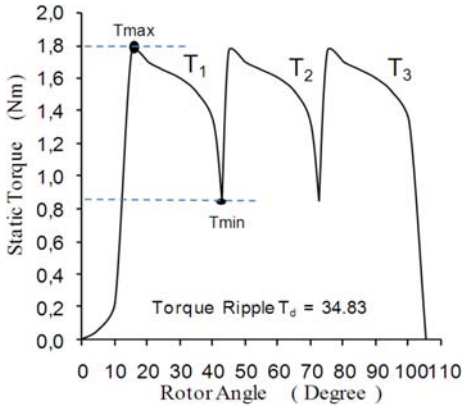

Figure 6

Static torques versus rotor angle (obtained from FEM) for three-phase and 10 A phase current

As is seen from the curve, the torque generated by the motor changes between about 1.8 Nm and 0.87 Nm for the 10 A phase current. In this case, the obtained static torque ripple is 34.83% (In Fig. 6, % torque ripple T_d = [(T_{max}-T_{min})/(T_{max}+T_{min})] x 100%).

The *L* values found by using FEM, as shown in Fig. 4, are used in the drawing of Fig. 5 and Fig. 6. One of the methods used to find the inductance (*L*) value is to measure it by using an instrument at each step while the rotor is rotating from 0° to 90° by 1° increments. In order to find the *L* value by means of this method, the motor should be physically manufactured. However, in this study, the motor is at the design stage. Therefore, all motor characteristics (inductance, current, flux, torque and speed, etc.) at the real working conditions of the motor that will be manufactured at given motor power, voltage and size (dimensions) values are found by using its Matlab- Simulink model. The main parameter of this model is the inductance. The *L* values at certain rotor angles between 0° and 90° (in this study, by 5° increments) should be known to the model in Matlab-Simulink. In this study, the *L* values are calculated by using FEM for certain rotor angles between 0° and 90°. Equations (4), (5) and (7) are used to calculate the *L* values.

But, the *L* values found by using FEM are valid for a certain moment (for example, for 5° rotor angle). In fact, under real working conditions, the parameters such as speed, current and torque values are a function of time and changing continuously. The static analysis that uses FEM cannot show the dynamic working since it only considers a certain moment and uses the values at this moment. In dynamic analysis, the electrical magnitudes of the motor at time varying work can be calculated by using the flux and inductance values obtained using FEM at certain current and position (angle) values. The Flux and inductance values are put into a lookup table whose inputs are *I* and θ. The interval values are obtained by using interpolation in this table.

2 Modelling of the SRM

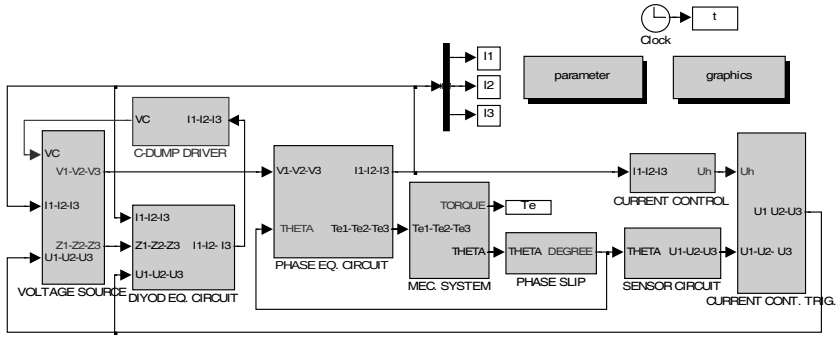

Figure 7
3-Phases SRM's linear model

The block scheme of the linear model generated by the dynamic equations given in Section I is given in Fig. 7. The model is comprised of the induced electrical torque for 3 phases, a C-dump driver circuit, a mechanical system, and a sensor circuit [11]. The block schemes, constituting the whole dynamic model, will be examined in this section.

2.1 One Phase Equivalent Circuit

From (2) and (3),

$$d\lambda/dt = V_s - R \cdot i_s \tag{8}$$

$$i_s = \lambda(\theta)/L(\theta) \tag{9}$$

The block scheme of one phase equivalent circuit obtained by means of (2) and (3) in Section I is given in Fig. 8.

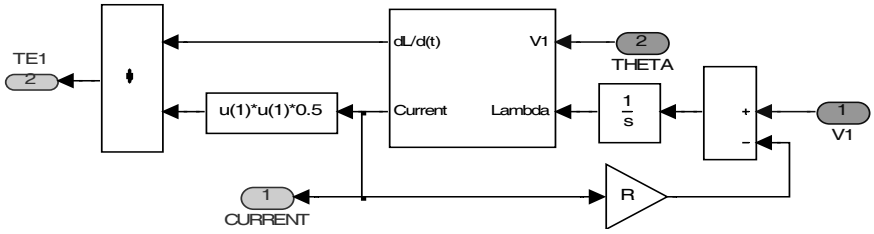

Figure 8
The block scheme of one phase equivalent circuit of SRM

The slope of inductance ($m = dL(\theta)/d\theta$) must be known in order to calculate the electrical torque expression in (6) for a certain phase current. Therefore, the inductance and its slope must be determined with respect to the variation of the rotor angle (θ) for a certain phase current. The inductance equation obtained by using FEM for the one phase and 8 A phase current is given in Table II.

As shown in Table II, the inductance values for the first phase can be divided into four linear regions as constant, increasing, decreasing and again constant region.

The increasing and decreasing regions are described as a line equation such as $L = m \cdot \theta - n_2$ for the increasing region and $L = - m \cdot \theta + n_3$ for the decreasing region.

The slope values are m = 0 for L_1 and L_4, m = 0.0091149 in radian and 0.000159 in degree for L_2 and L_3; the constant values in radian and in degree are N_2 = 0.001428 and N_3 = 0.012888 for the 8 a phase current. In practice, the rotation angle is used in degrees. therefore, 0.000159 degree is used instead of 0.0091149 radian in the model since the degree unit is preferred in the matlab-simulink model.

Table II

The linearized equation determined with respect to θ for one phase and 8 A phase current

	$L(H)$		θ
	(θ = Degree)	(θ = Radian)	
L_1	L_{min}=0.00056	L_{min}=0.00056	0.0°≤ θ ≤ 12.5° (0.0 rad.≤ θ ≤ 0.2182 rad.)
L_2	0.000159*θ – 0.001428	0.0091149*θ – 0.001428	12.5°≤ θ ≤ 45.0° (0.2182 rad.≤ θ ≤ 0.7854 rad.)
L_3	-0.000159*θ + 0.012888	-0.0091149*θ + 0.01288	45.0°≤ θ ≤ 77.5° (0.7854 rad.≤ θ ≤ 1.3526 rad.)
L_4	L_{min}=0.00056	L_{min}=0.00056	77.5°≤ θ ≤ 90.0° (1.3526 rad.≤ θ ≤ 1.5708 rad.)

The circuit model identifying the slope and the inductance value for the first phase of the motor is given in Figs. 9 and 10.

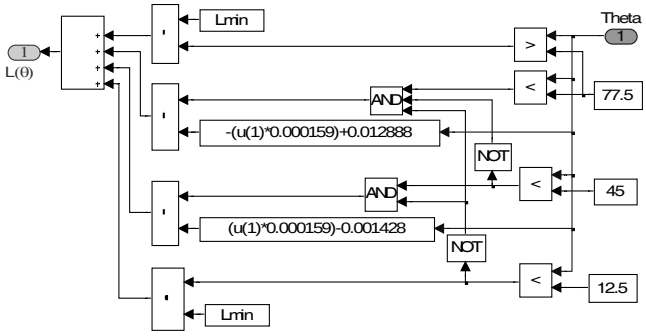

Figure 9

The circuit model identifying the value of the inductance for the first phase of the motor

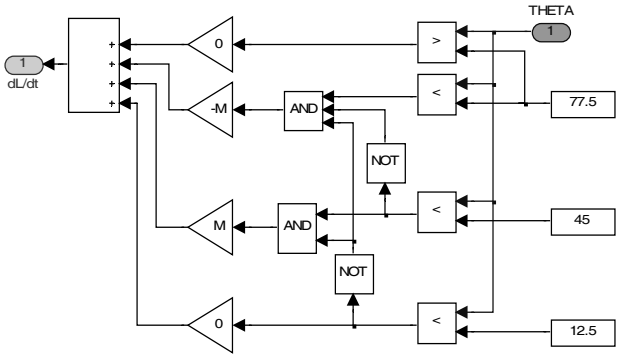

Figure 10

The circuit model identifying the inductance slope ($m=dL(\theta)/d\theta$) for the first phase of the motor

2.2 Mechanical Equivalent Circuit and Determining of the Rotating Angle

One of the expressions linking the electrical and mechanical sides of the motor is the torque expression given in (10), and the other is the acceleration expression of the rotor given in (12).

$$T_e = T_l + T_f + T_j \tag{10}$$

$$T_l = k_l \cdot \omega^z \;\; ; \;\; T_f = k_f \cdot \omega \;\; ; \;\; T_j = J \; d\omega/dt \;\; ; \;\; \theta = \omega \cdot t \tag{11}$$

where T_e is the electrical motor torque, T_l is the load torque, T_f is the friction or mechanical damping torque, T_j is the inertia torque, k_l is the load constant, k_f is the friction or mechanical damping constant, J is the inertia constant, θ is the rotor position angle, ω is the angular speed and z is the load coefficient, which changes between -1 and 2. The value z is taken as 1 in this study. Thus, the formula for the angular acceleration is derived as

$$d\omega/dt = [T_e - (k_l + k_f) \cdot \omega]/J \tag{12}$$

If the above acceleration expression is successively integrated twice, the rotor position angle can be obtained. This (θ) angle is used to determine the inductance and the slope of inductance and the driving of the SRM phase switches as power electronic components. The equivalent simulink scheme obtained by using (12) is given in Fig. 11.

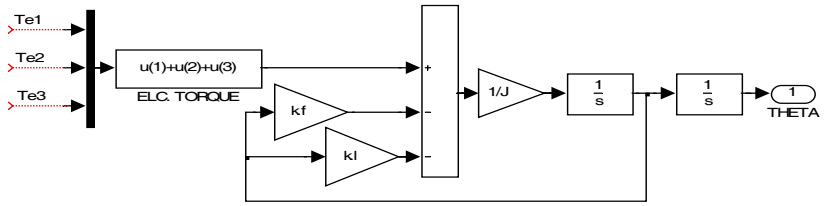

Figure 11
SRM's mechanical equivalent circuit scheme

Each phase winding of the SRM is supplied through power switches so that their conduction (dwell) angles are controlled according to the rotor position of the motor. For this purpose, three sensors are installed on the motor axle to obtain instantaneous (θ) position data, which is calculated as (θ) function by means of the circuit given in Fig. 11. The conduction angles of the semi-conductor switches (for U1, U2, U3) driving the phase windings is respectively shown in Fig. 12. Since the analyzed SRM has three phases, the conduction angle of each phase is 32.5° [4].

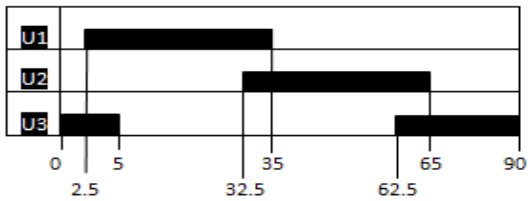

Figure 12
Conduction angles for three phases

2.3 C-Dump Driver Circuit

In the simulation of the SRM, a C-Dump converter is used as a drive circuit. Only one power switch is employed to drive each phase winding of the motor in the C-Dump converter. Since minimum number of switches are needed to supply phase currents in C-Dump converters [12], the C-dump converter is preferred in this study. From the C-Dump driver circuit,

$$dV_c/dt = (I - U_g \cdot I_g) / C_r \tag{13}$$

$$dI_g/dt = (U_g \cdot V_c - V_s - R_g \cdot I_g) / L_g \tag{14}$$

where V_c is the C-Dump voltage (V), V_s is the winding voltage (V), U_g is the constant determined the position of C-dump driver circuit switch (as 1 or 0), I is the total phase current (A), I_g is the C-dump current (A), R_g is the C-dump resistance (Ω) and L_g is the inductance of the C-dump circuit (H). The C-dump driver circuit obtained by means of Eqs. 13 and 14 is shown in Fig. 13. In Fig. 13, Z_g is the impedance of diode used in the C-dump driver circuit (Ω).

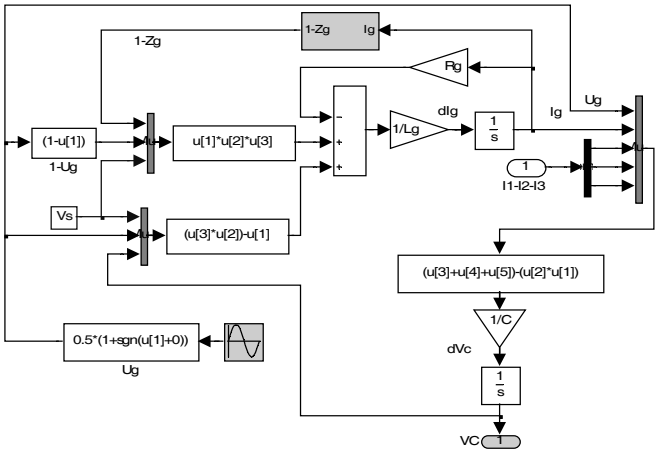

Figure 13
C-Dump driver circuit

3 Simulation Results and Discussions

The characteristic curves of the rotor position, speed, inductance, current, torque and flux obtained by the simulation of the 6/4 SRM's dynamic model given in Fig. 1 are presented in this section. The rotor position angle versus time is given in Fig. 14.

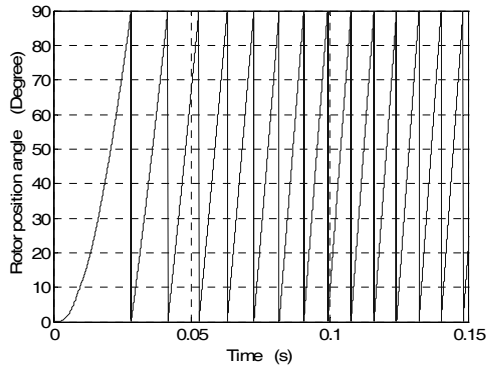

Figure 14
Rotor position angle versus time

As seen from Fig. 14, the period of the rotor position is 90° in 6/4 SRM and the rotor motion from one pole to the other is slow at the beginning, and then it starts to accelerate. The motor speed versus time is given in Fig. 15.

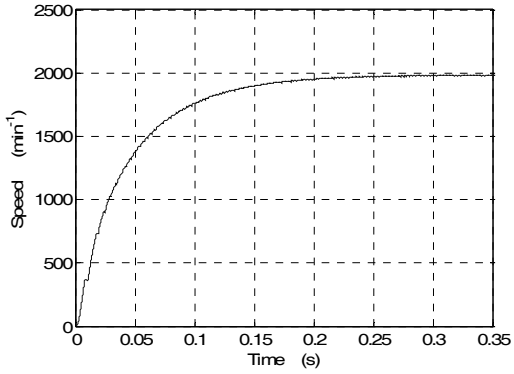

Figure 15
Motor speed versus time

As seen from Fig. 15, the speed of the SRM reaches to the nominal speed of 2000 rpm from 0 within 0.35 seconds after the starting time and comes to a stable condition. The dynamic phase inductances versus time are illustrated in Fig. 16.

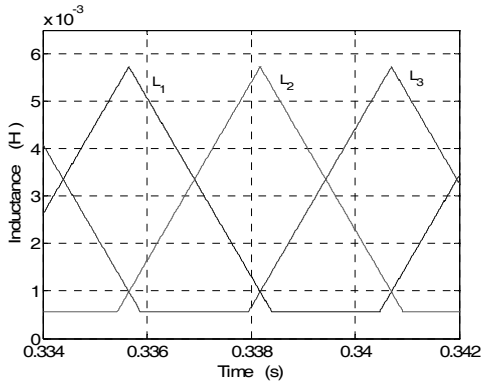

Figure 16
Dynamic phase inductances versus time

As seen from Fig. 16, the value of every phase inductance changes between 5.73 mH and 0.56 mH. These values are equivalent to the static inductance values at about the 8 A phase current. The phase currents versus time are given in Fig. 17. During the conduction angle, the phase currents rise to 17.6 A and finally fall to 8.3 A. If no current limiting protection is applied to the motor, these 17.6 A phase currents may be dangerous for the motor windings. Therefore, these currents must be restricted to a certain level.

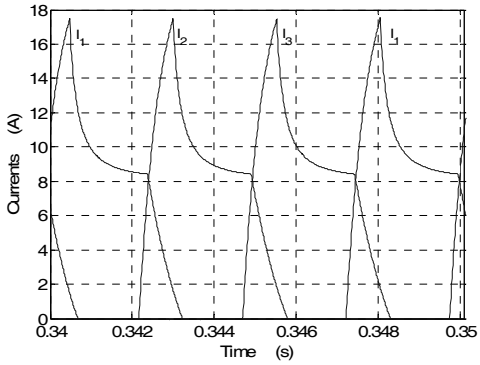

Figure 17
Phase currents versus time

Within the scope of this study, another analysis is also carried out, on in which the phase current is controlled and limited, and the simulation results are compared with those of the unlimited control model. As seen from Fig. 17, the phase currents cross at 8 A, which is the minimum phase current of the SRM. This current value is valuable for designing the driver circuit components since this crossing means that the phase current of the SRM must be 8 A.

When one phase is switched on, the previous phase that is switched off does not immediately show zero current. However, it is desired that it be zero. Therefore, using a C-Dump circuit, this current should be rapidly brought to zero by applying reverse voltage to the phase that is switched off.

The dynamic torque-time characteristics of the SRM are seen in Fig. 18. It is seen that the maximum torque on these curves is 1.33 Nm on this curve and the torque generated by the motor per phase changes between 1.33 Nm and 0.015 Nm periodically. This variation with the sharp wave form shapes in torque causes undesired vibrations and acoustic noise in the motor. The average torque of the SRM is 0.3 Nm.

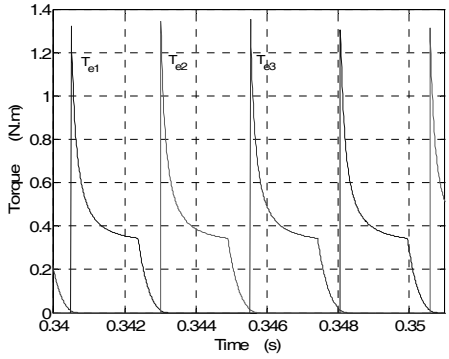

Figure 18
Dynamic torques versus time

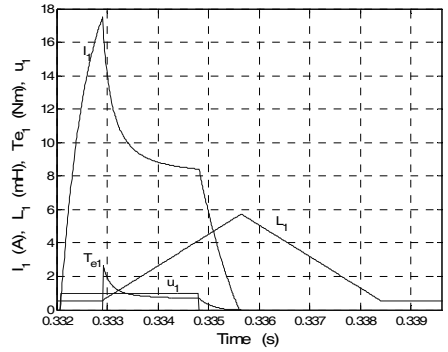

Figure 19
Inductance (L_1), current (I_1), torque (T_{e1}) versus time and conduction times (u_1) for first phase of SRM

To understand the dynamic analysis results better, the inductance, current, torque versus time and conduction times for one phase are illustrated as a whole in Fig. 19. In these curves, the current and inductance values are plotted with their real values, but the torque values are enlarged by 2 to make it clearer.

As can be seen in Fig. 19, the increasing and decreasing of the inductance is symmetric and linear. When the phase winding current is switched off in the increasing region of the inductance, the current rapidly decreases. The current is rapidly brought to zero by applying reverse voltage to the phase winding that is switched off by means of the C-Dump circuit at the end of conduction time. While the motor does not produce the torque in the region where the inductance is constant in Fig. 19, it produces the torque depending on the value of phase current in the increasing region of inductance. On the other hand, the phase flux of the motor increases rapidly in the increasing region of the current. And it continues to increase linearly from the point where the current starts to decrease (the point where the inductance starts to increase) until the end of the conduction time.

At the end of the conduction time, it decreases parallel to the decrease in the current and becomes zero simultaneously with the current. The torque generated by the SRM should remain as stable as possible. Since the torque is proportional to the square of the phase current, the motor current should remain constant at a certain value. In practice, the current control is applied to keep the phase current constant at a certain value in the motor control circuit [13].

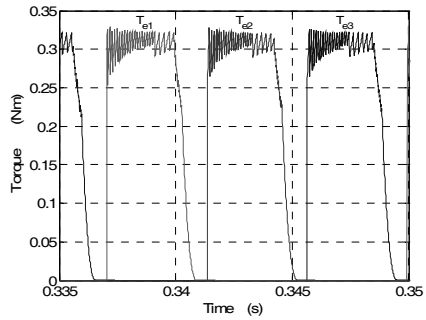

Figure 20
8 A current controlled dynamic torques versus time

The simulated dynamic torques versus time with current control at 8 A are given in Fig. 20. The average torque of the SRM becomes 0.25 Nm and 75% improvement in torque ripple is obtained when the current control is applied to the motor at 8 A, as is shown in Fig. 20. The flux variation versus phase current for one phase of the SRM's dynamic model simulation is given in Fig. 21. When the flux versus current curves (in Figs. 2 and 21) are compared, it is seen that the flux for one phase obtained by dynamic analysis at the 8 A phase current (Fig. 21) is 30.5 mWb, whereas the flux for one phase obtained by using FEM (Fig. 2) is 14.33 mWb for $\theta = 45°$. The curves in Fig. 2 don't exactly conform with the curves in Fig. 21 because of the linearization of the inductance profile. When the motor phase current is controlled at 8 A, the torque and phase currents versus time for the studied SRM are presented in Fig. 22. It is obvious that a 75% improvement is achieved in the torque ripple of the current controlled model.

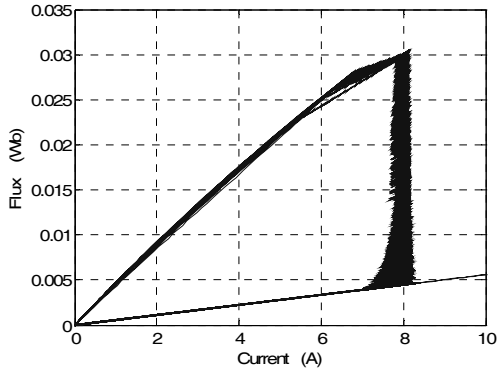

Figure 21

Flux variations versus current for one phase obtained by the result of SRM's dynamic model simulation

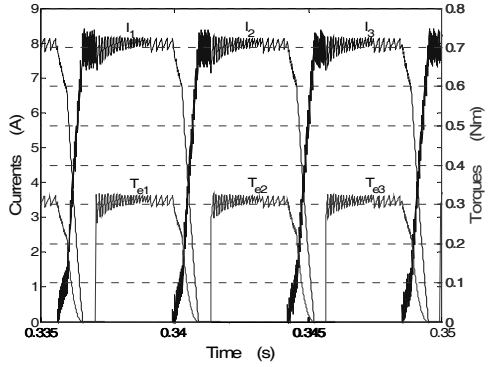

Figure 22

8 A current controlled dynamic torque and phase current versus time

Conclusions

In the article, a computer-based matlab-simulink modelling was presented to supplement the teaching of modelling subjects. The modelling allows learners to see the results of analysis and the possible remedial action. The program provides a better understanding of the SRM's dynamic behaviour and remedial action without the need to perform time consuming hardware experiments, which are also expensive to set-up.

In this study, the results obtained from the linear dynamic analysis of an SRM may be summarized as follows:

- The value of the current through the phase windings and the conduction angles are important criteria for drive design in the linear model of the SRM. Since the phase winding currents are controlled via power electronic switches, the peak

value of the current through the windings must be determined before any control.

- In this study, 97.77% torque ripple is seen in the case of the dynamic analysis without current control, although the static torque ripple for only 10 A is examined and 34.83% torque ripple is achieved in the study of [10]. The reduction in torque ripple is observed when the motor phase current is controlled at 8 A.
- In static analysis, the torque produced by the SRM becomes 1.8 Nm while the current of 10 A flows through the phase windings. On the other side, in dynamic analysis without current control, the produced torque becomes max. 1.33 Nm while the max. 17.6 A current flows through the phase windings and the maximum torque of 0.3 Nm is obtained when the phase current of the motor is controlled at 8 A. Moreover, the linear dynamic analysis determines the torque that will be produced by the motor. That is, it determines the dynamic behaviour of the motor. In order to examine the motor in more detail, a non-linear analysis may be needed.

Appendix

The main definition for inductance is $L = N \cdot \Phi / I$. An equivalent definition for inductance may be made using an energy point of view,

$$L = \frac{2W_m}{I^2} \tag{15}$$

where I is the current flowing in the stator winding and W_m is the energy in the magnetic field produced by the current. If the potential energy W_m is expressed in terms of the magnetic fields,

$$L = \frac{\int_{vol} B \cdot H \cdot dv}{I^2} \tag{16}$$

and replace B by $\nabla x A$

$$L = \frac{1}{I^2} \int_{vol} H \cdot (\nabla x A) \cdot dv \tag{17}$$

The vector identity

$$\nabla \cdot (A x H) \equiv H \cdot (\nabla x A) - A \cdot (\nabla x H) \tag{18}$$

may be proved by expansion in cartesian coordinates. The inductance is then

$$L = \frac{1}{I^2} \left[\int_{vol} \nabla \cdot (A x H) \cdot dv + \int_{vol} A \cdot (\nabla x H) \cdot dv \right] \tag{19}$$

After applying the divergence theorem to the first integral and letting $\nabla x H = J_i$, we have

$$L = \frac{1}{I^2}\left[\oint_S (A x H)\cdot dS + \int_{vol} A \cdot J_i \cdot dv\right] \tag{20}$$

Since the surface encloses the volume containing all the magnetic energy, the surface integral is zero, which requires that A and H also be zero on the bounding surface. The inductance may therefore be written as

$$L = \frac{1}{I^2}\int_{vol} A \cdot J_i \cdot dv \tag{21}$$

where A is the vector magnetic potential (Wb/m) and J_i is the current density (A/m^2) [14].

References

[1] T. J. E. Miller: Switched Reluctance Motors and Their Control, Magna Physics Publishing Press, Oxford University, USA, 1993

[2] P. J. Lawrenson, J. M. Stephenson, P. T. Blenkinsop, J. Korda, N. N. Fulton: Variable-Speed Switched Reluctance Motors, Electric Power Applications (IEE Proceedings B), Vol. 127, Issue 4, July 1980, pp. 253-265

[3] G. S. Buja, M. I. Valla: Control Characteristics of the SRM Drives-Part I: Operation in the Linear Region, IEEE Trans. Ind. Electron., Vol. 38, 1991, pp. 313-321

[4] D. A. Torrey, J. H. Lang: Modelling a Nonlinear Variable Reluctance Drive, 5th European Conference on Power Electronics and Applications, Brighton, U.K, 1993

[5] G. S. Buja, M. I. Valla: Control Characteristics of Switched Reluctance Motor Drive Taking into Account the Motor Saturation, IECON '90, 16th Annual Conference of IEEE, Pacific Grove, California, USA, 1990

[6] V. F. Ray, P. J. Lawrenson, R. M. Davis, J. M. Stephenson, N. N. Fulton, R. J. Blake: High Performance Switched Reluctance Brushless Drivers, IEEE Trans. Ind. Appl., Vol. 1A-22, No. 4, 1986, pp. 722-729

[7] M. R. Harris, J. W. Finc, J. A. Mallick, T. J. E.Miller: A Review of the Integral Horsepower Switched Reluctance Drive, IEEE Trans. Ind. Appl., Vol. 1A -22, No. 4, 1986, pp. 716-722

[8] F. Soares, P. J. C. Branco: Simulation of a 6/4 Switched Reluctance Motor Based on Matlab/Simulink Environment, IEEE Trans. on Aerospace and Electronic Systems, Vol. 37, No. 3, 2001, pp. 989-1009

[9] S. Sadeghi, M. Mirsalim, A. H. Isfahani: Dynamic Modeling and Simulation of a Switched Reluctance Motor in a Series Hybrid Electric Vehicle, Acta Polytechnica Hungarica, Journal of Applied Sciences, Hungary, Vol. 7, Issue 1, 2010, pp. 51-71

[10] Y. Özoğlu: Anahtarlamalı relüktans motorunda kutup başlarına şekil vererek moment dalgalanmasının azaltılması, Ph.D. dissertation, Dept. Electrical Eng., İstanbul Tech. Univ., İstanbul, Turkey, 1999

[11] H. Çalık: Control of the Switched Reluctance Motor, Ph.D. dissertation, Dept. Electrical Edu., Marmara Univ., İstanbul, Turkey, 2005

[12] V. Özbulur, M. O. Bilgiç, A. Şabanoviç: Torque Ripple Reduction of Switched Reluctance Motor, IEEJ-1995 International Power Electronics Conference, Yokohama, Japan, 1995

[13] S. Vukosavic, R. Stefanovic: Switched Reluctance Motor Inverter Topologies: a Comparative Evaluation, IEEE Trans. Ind. App., Vol. 27, No. 6, 1991, pp. 1034-1047

[14] Jr. W. H. Hayt: Engineering Electromagnetics, McGraw-Hill Kogakusha Ltd., 3rd Ed., 1974